

Detection of invisible SPM distribution in the sky

Toru YAGI¹⁾ Junko KAMBE¹⁾ Tomoo AOYAMA¹⁾

Abstract

Suspended Particulate Matter (SPM) is dusts in the atmosphere, which exists from ancient times. Nowadays, they have two origins that are natural and artificial. The diameter is distributed between 1 ~ 10 μm. Natural SPM is almost soil particles, and includes bacteria and virus on the surfaces. Artificial SPM is industry by-products; *that is*, complex matters over one hundred kinds of compounds. Even if SPM is under the gravity, the falling speed is negligible, and it moves as well as the gas.

As property of small particles, it attracts many substances. If SPM moves through polluted air, it transports contamination matters towards leeward. The phenomenon is found beyond countries. An example is the yellow sand arising from Taklamakan desert flows until Greenland. SPM is a meteorological word. We hear it as “PM2.5” in various media.

Very concentrated SPM makes the sky be cloudy. The phenomenon is not found yet in Japan. Existence of dilute SPM is detected as hazy sky, which degree is small. Therefore; we detect the haze by using digital cameras. We have observed the SPM at Norikura observatory from 2011 until 2016. This is a report of the digital measurements and discussions of the image processing. Where, conception of physical color, meaning of color-ratio, contouring image approach as extraction of character of targets, two dimensional Fourier Transformation are discussed.

Figures are drawn by using full color. The true images will be got from Web-pages.

Keywords: Suspended Particulate Matter, PM2.5, haze, Norikura observatory, digital camera, physical color, color-ratio, contour map, Fourier Transformation

1. Introduction

Water drops are condensed around SPM in the atmosphere, and they are grown in turbulence, and make clouds [1]. The process is done in supersaturation of moisture. Contrary, water drops are evaporated in unsaturated air, and returned to dust. The dust is diffused and makes black mist layers. The dynamics are found at the top of cumulus.

We observe the black layers and cumulus at Marishiten peak (2872m) in Norikura, from 2011 until 2016, and analyze the spectrum by using digital cameras [2].

2. Theory of color ratios

In a RAW format, the color is expressed by $F(x,y;r,g,b)$, where $\{x,y\}$ is the location of pixels of images, and $\{r,g,b\}$ is a color-intensity in interval of $[0,2^n-1]$. The n is 8 (sRGB [3] space): *that is*, human’s visual recognition. Now, digital camera has $n \sim 14$. Thus; the camera has a potential of huge color world beyond human being. *We wish to search the world and get new recognition for suspended*

dusts in the atmosphere.

The $\{r,g,b\}$ corresponds outputs of detected photodiodes, and the wavelength intervals are $[400,500]$, $[500,600]$, $[600,650]$ in [nm]. It is not $\{r,g,b\}$ in Jpeg-format [4], in which Jpeg- $\{r,g,b\}$ is transformed from RAW- $\{r,g,b\}$ by using 3×3 matrix (The function is in our thesis, “Two dimensional Fourier Transformation”).

Small particles in the atmosphere scatter the light, and wavelength depends on the diameters. The wavelength dependency is expressed as λ^{-n} , where λ is wavelength [nm], and n is Angstrom coefficient [no dimension] [5]. The n is changed continuously from 4 (fine sky) until 0 (cloudy). The $n=4$ is emitted by Rayleigh scattering of air molecules, and $n=0$ is done by Mie scattering of small particles about 1 ~ 10 [μm]. Diameter of rain drops are greater than 20 [μm]. SPM is environmental contaminations, which are classified PM10 and PM2.5 by distribution center point of the diameter. SPM is complex of many substances, and it gives Mie scatters. The scattering spectrum is unknown. We observe concentrated SPM as a black mist layer, empirically. On considering the empirical situations, SPM would have a broad absorption band. To detect the SPM from images got from digital cameras, we adopt B/R-ratio. The ratio is quotient of each intensities of $\{r,g,b\}$; *i.e.*, $\{b/g,r/b,r\}$.

Here, we get $F(x,y;b/r;g/r;b/g)$ from $F(x,y;r,g,b)$. The ratios

are small vales that must be normalized,

$$F'(x,y,b/r)=(2^8-1)(F(x,y,b/r)-x_{min})/(x_{max}-x_{min}),$$

$$x_{max}=\max(F(x,y,b/r)), x_{min}=\min(F(x,y,b/r)),$$

same as g/r and b/g . (1)

We set correspondence between $\{b/r, g/r, b/g\}$ and $\{b,g,r\}^*$.

The coloring indicates density of suspended particulate matter in the atmosphere [6]. $F'(x,y,b/r,g/r,b/g)$ is free for optical-dimming of photodiode detector arrays. It is a superior point to amplify the images for searching hidden phenomena.

*) The ordering has not physical meanings. In detecting the sky conditions, the most sensitive ratio is b/r empirically. Therefore, it is set first element of vector-representation. The b/g has less information as detector index; then, the element is the last.

3. Contour Operator

Considering following operation,

$$F_s(x,y)=[d^{-1}[d F(x,y)]], 0<d<1, (2)$$

Where $[]$ is Gauss symbol (round down decimal places), and $F_s(x,y)$ is integer. This is a step-function by parameter d . Therefore, next IF-processing makes a contour.

$$\text{IF } F_s(x,y)=F_s(x+1,y) \ \& \ F_s(x,y)=F_s(x,y+1) \ \text{THEN} \\ G(x,y)=255; \ \text{ELSE } G(x,y)=0; (3)$$

If $F(x,y)$ doesn't include noises, Eq. (3) makes contours. It is confirmed following section.

4. Test for detection of dilute SPM as a model

We define an ideal sky based on wavelength dependency of Rayleigh and Mie scattering.

Scattering intensity functions of blue, green, and red are

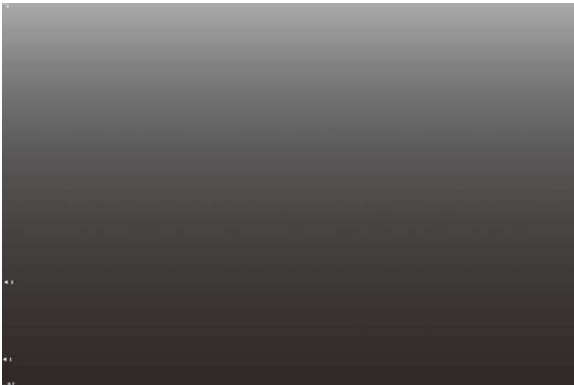


Figure 1: Image of an ideal sky.

Table 1: Relation of $b/r, g/r, b/g$ ratios and n -parameter

n	b/r	g/r	b/g
4.0*	3.72	1.67	2.23
3.0	2.68	1.47	1.83
2.5	2.27	1.38	1.65
2.0	1.93	1.29	1.49
1.5	1.64	1.21	1.35
1.0	1.39	1.14	1.22
0.50	1.18	1.07	1.11
0.25	1.09	1.03	1.05
0.0**	1.00	1.00	1.00
-0.25	0.92	0.97	0.95

*) complete fine day, **) cloudy

expressed as $b(n), g(n),$ and $r(n)$. Using the center wavelength $[\mu\text{m}]$ of each color, we get,

$$b(n)=1/0.45^n, g(n)=1/0.55^n, r(n)=1/0.625^n, (4)$$

Using Eq. (4), the relation of b/r -ratio and n -parameter is evaluated; the result is listed in Table 1.

Horizontal lines are drawn by the color of λ^n (λ is wavelength, $0.4\leq\lambda\leq0.625$ $[\mu\text{m}]$, $-0.75\leq n\leq 4$). The $n=4$ and $n=0$ correspond with pure Rayleigh and Mie scattering. Figure 1 is developed 8-bits linear color; non-linear translation is not processed for a dark-part. From top to bottom lines, the mixing ratio of Rayleigh and Mie scattering is changed continuously.

The origin information (as for intensities calculated by λ and n directly) is hold in 32-bits. We add various dust information to the origin data. An example is in Figure 2. Parameters of scattering wavelength of SPM are $n=1.75$ and $n=1.5$, which are upper and lower. The scattering light is both blue in our sense. The 33% of Figure 2 is added on 67% of Figure 1. Weak blue spots are overlapped on dark blue background of Figure 1; therefore, no change is detected.

It is a same image of Figure 1. Images of SPM cannot be

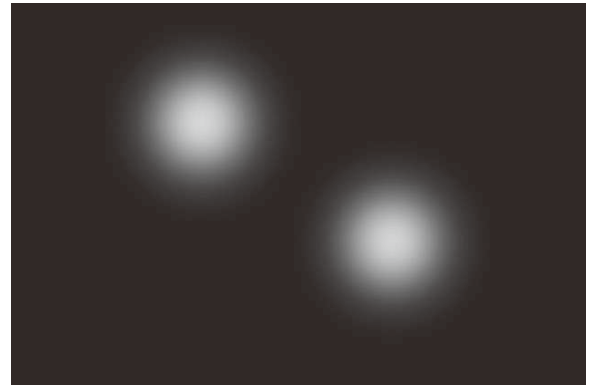


Figure 2: SPM scattering image that is added to Figure 1.

seen naturally. Concentrated SPM makes blue sky be hazy. The situation is known as Yellow sand. This is a model as for natural SPM. The contour approach is effective to detect extremely thin images. That is shown in Figure 3.

Where, we adopt $d=0.5$ in Eq. (2), and normalize B/R image by Eq. (1). Invisible two SPM are detected clearly*. Continuous change of character of scattering light is confirmed by contour intervals.

) A color $\{x\}=\{r,g,b\}$ can be emphasized by expressions, $255(x-x_{min})/(x_{max}-x_{min})$, or $\text{bias}*x+\text{base}$. The approaches give continuous images. Field images include noises; therefore, the noises are emphasized also, So images with granular are got. Contour approach suppresses the noises, but the function is not so powerful. Even if the approach is adopted, noise traces are found as crinkly lines. In case of this model calculation, there is no noise; therefore, the contour curves are smooth and moiré is arisen.

Contour map of section 3 is effective in a model case that doesn't noise; on general cases in the fields, however, the map is drawn by dots, and gives broad bands.

5. Color in RAW format

RGB values in RAW format of digital cameras are " $r(x,y), g(x,y), b(x,y)$ ", which has locations (x,y) in pixel unit*. The maximum values, " $\text{Max}\{r(x,y)\}, \text{Max}\{g(x,y)\}, \text{Max}\{b(x,y)\}$ ", have wavelength dependency of scattering of a most bright target. If " $r(x,y), g(x,y), b(x,y)$ " of a fine sky are not relation: " $b(x,y) > g(x,y) > r(x,y)$ **", the RAW data is not got under the sun. Or unpublished processing is done in firmware.

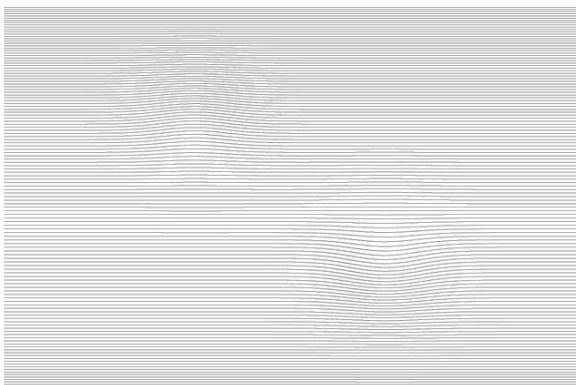


Figure 3: Contour map of B/R-monochrome image of SPM in ideal sky. SPM image has moiré.

*) In case of direct access for Bayer's array in RAW format, 4 elements correspond to 1-pixel. The 4 elements have $\{r;g0; b,g1\}$ information, and the locations are different slightly. On such a condition, the expression is very complex. To simplify them, we make Bayer's array be 1-location (x,y) , and $\{r,g,b\}$ -information. Where, $(x,y)=\{(r+g0)/2+(b+g1)/2\}, \{(r+b)/2+(g0+g1)/2\}/2$, and $\text{Intensity}(g)=\text{Intensity}(\{g0+g1\}/2)$. Those are represented by $r(x,y), \dots$ etc.

**) The light from the sky is intermediate character between Rayleigh and Mie scattering. The wavelength depends on " $\lambda^{-n}, 4 > n > 0$ ". The condition of " $b(x,y) > g(x,y) > r(x,y)$ " is required.

If you wonder the firmware, a condition may be introduced in restriction of sky images.

$$M = \text{Max}[\text{Max}\{r(x,y)\}, \text{Max}\{g(x,y)\}, \text{Max}\{b(x,y)\}],$$

$$F = \text{Max}\{b(x,y)\}/M,$$

$$b'(x,y) = b(x,y)F,$$

$$g'(x,y) = g(x,y)F\{0.55^n/0.45^n\},$$

$$r'(x,y) = r(x,y)F\{0.625^n/0.45^n\}, \tag{5}$$

The " $r'(x,y), g'(x,y), b'(x,y)$ " has same wavelength dependency as that of Eq. (4). We rewrite Eq. (5) $F(x,y; r',g',b') := F(x,y,r,g,b)$. We use the $F(x,y,r,g,b)$. Partial set $\{F(x,y,r)\} \subset F(x,y,r,g,b)$.

Under assuming n-parameter of target sky, a compensation image is obtained. We get deep blue, blue, hazy blue, bluish gray, magenta gray skies for $n=\{3, 2, 1, 0.5, 0.0\}$, respectively.

Under the compensation image $\{r'(x,y), g'(x,y), b'(x,y)\}$, color ratios are recalculated. So, we get,

$$4 > \text{Max}\{b'(x,y)/r'(x,y)\} > 1 > \text{Min}\{b'(x,y)/r'(x,y)\} > 0.$$

$$\text{Norm}(x,y) = 127.5 / \text{Max}[\text{Max}\{b'(x,y)/r'(x,y)\} - 1,$$

$$1 - \text{Min}\{b'(x,y)/r'(x,y)\}],$$

$$(\text{B/R})\text{image} := 128 + \text{Norm}\{(b'/r')(x,y)\}, \tag{6}$$

Same as the derivation, (G/R) and (B/G) images are got. Eq. (6) is used to compare broad spectrum of the dust. Therefore, a middle point (=128) bias is introduced.

6. Applied to volcano Gas of Yakedake

Yakedake (2455m) is an active volcano in Nagano, and exhausts moisture and gas. The high temperature exhaust is cooled, and generates water drops, which scatters the light. Then, we can see them. The water drops attracts volcano gas, and may have very thin color. We research



Figure 4: Exhaust gas of Yakedake.

the drops by photographic approach. The $F(x,y,r,g,b)$ image is Figure 4, whose tone is linearly projected into 8-bits. It has no color, and is white visually by scattering. To research terminus of the exhaust, we adopt contour approach of $d=0.2$ for monochrome term $F_M(x,y)$.

$$F_M(x,y) = \{F(x,y,r) + F(x,y,g) + F(x,y,b)\} / 3. \quad (7)$$

The $F(x,y,r)$ is the partial set of $F(x,y,r,g,b)$. The $F_M(x,y)$ is in Figure 5.

It is photographed at 8:30 JST, 2014.9.2, by using Nikon D7100, 1/3000 s, ISO=400, Nikkor 50mm F6.7.

It is physical linear tone image, and the color is $\{r,g,b\}$. By using Eq. (5), monochrome image $F_M(x,y)$ is generated. From the $F_M(x,y)$ and parameter $d=0.2$, Figure 5 is generated.

Where, d of Eq. (2) is 0.2. It is visualized that the exhaust makes turbulence, and the terminus reaches to neighborhood peak.

Figure 5 isn't no longer contour image. It is a reason why noises exist and make a lot of dots. IF-statement in Eq. (5) has a weak point for noises. To eliminate noises from target image, we adopt following Fourier Transformation.

7. Two dimensional Fourier ransformation

Theory of Fourier Transformation (FT) is published [7].

A continuous function $F(t)$ is expanded by the orthonormal set. Triangular functions $\{\sin(nt), \cos(nt); n=0,1,\dots,\text{integer}\}$ is the set. $F(t) = \sum_0^{\infty} \{An \sin(nt) + Bn \cos(nt)\}$,

$$An = \int F(t) \sin(nt) dt, \quad Bn = \int F(t) \cos(nt) dt. \quad (8)$$

By sampling theory [2], Eq. (8) is reduced,

$$F(t) = \sum_0^N \{An \sin(nt) + Bn \cos(nt)\},$$

$$A0 = 0, \quad 2B0 = \int_0^{2\pi} F(t) dt, \quad 0 \leq t \leq 2\pi,$$

$$\pi An = \int_0^{2\pi} F(t) \sin(nt) dt, \quad \pi Bn = \int_0^{2\pi} F(t) \cos(nt) dt, \quad (9)$$

Where \sum_0^N runs over n , and N is $<$ sampling number/2.

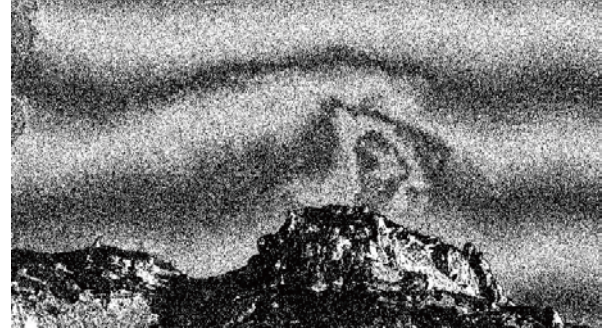


Figure 5: Contour image of Figure 4.

Eq. (9) is rewritten as for 2D.

$$F(x,y) = \sum_0^N \sum_0^M \{An \sin(nx) + Bn \cos(nx)\} \\ \times \{Cm \sin(my) + Dm \cos(my)\}. \quad (10)$$

Since N and M of images are $3k \sim 5k$, a calculation of Eq. (10) requires large CPU. In restricted CPU, We adopt important lower triangular part of summation. And N is limited under 700.

$$F(x,y) \sim \sum_0^N \sum_0^M \{1 - \delta(N+M, Nq)\} \{An \sin(nx) + Bn \cos(nx)\} \\ \{Cm \sin(my) + Dm \cos(my)\}, \quad Nq = \max(0, 1, \dots, N), \\ \delta(N+M, Nq) = \{0(N+M \leq Nq); 1(\text{otherwise})\}, \quad (11)$$

Using Eq. (11), a small area is transformed; therefore, the corners and sides must be zeros. Then, we introduce a window. However, since ordinary window [8] deforms the center part of images, we adopt local window operated the terminal parts.

At first, the width of a window x_L is defined as $0 \leq x \leq x_L = 20\delta x$. The δx corresponds a pixel, and the number (20) is determined experimentally under allowable deformation of transformed image.

New a variable t is defined. $0 \leq t \leq \pi/2$. The relation is, $t = (\pi/2)/x_L$. The window is, $W_L(t) = \sin(t)$, which operates image-terminal in $[0, x_L]$. This is left-side window; at same way, right-, upper-, lower-sides windows are got. Size of Fourier Transformed image is $N \times M$ pixels, the result image is $(N-40) \times (M-40)$ pixels under using windows. An example of Figure 4 is displid.

It shows details of dilute part of volcano exhaust, moreover, noises are suppressed about 1/10. Therefore, contour is displayed by lines.



Figure 6: Two dimensional Fourier Transformed image of Figure 4. This is monochrome. Target area is 721×721 pixels, and expansion waves are 70 for one dimension.

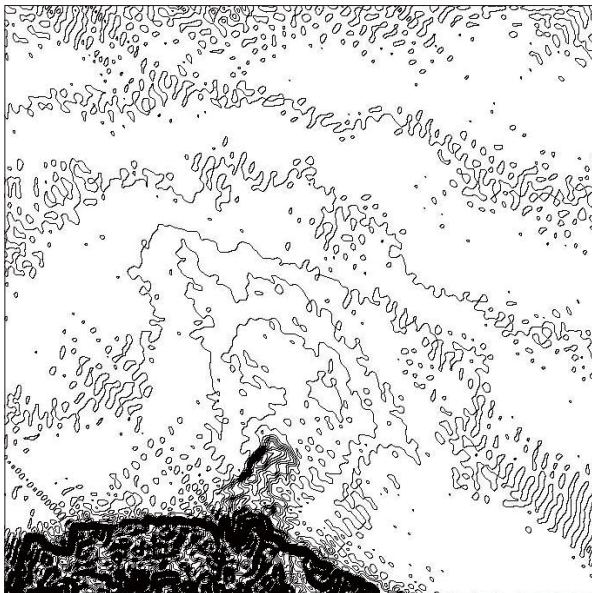


Figure 7: Contour map of Figure 6, in case of $d=0.2$.

8. Colors of volcano exhaust

To investigate color of the exhaust, we calculate 3 images of $F'(x,y,b/r)$, $F'(x,y,g/r)$, and $F'(x,y,b/g)$, where $n=0.5$. The images are very flat, and no pattern is. To get images, we extract square region of 333×334 pixels and make images normalize in $[0, 2^8-1]$; so we get Figure 8. After the calculations, we execute same processing by using $n=\{1, 3\}$. It is to confirm “no exhaust pattern” doesn’t depend on the selection of n -parameter. As the results, we get none.

Figure 8: From top to bottom, $\{b/r; g/r; b/g\}$ -image of exhaust gas of Yakedake. Intensity of images is amplified by 5 times. All levels of ratio=1 are 127.5 in 255 steps.

The exhaust gas looks non image in $\{b/r\}$, and does

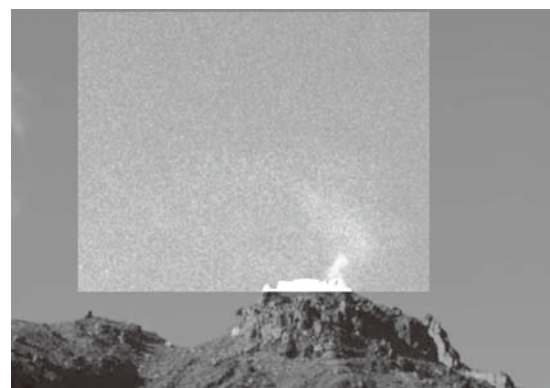
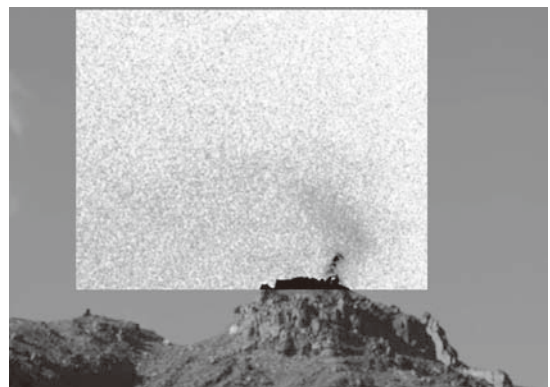
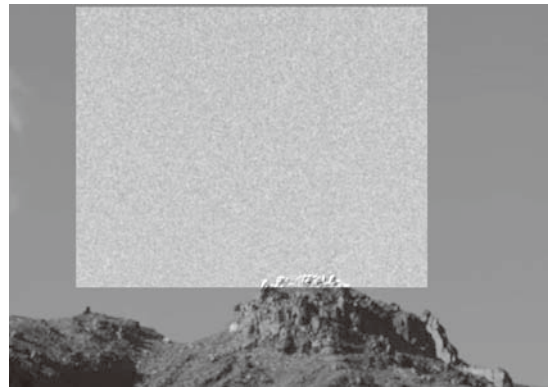


Figure 8: Exhaust gas of Yakedake.

black in $\{g/r\}$. It indicates $b>g$ based on r -light. $\{b/g\}$ image indicates white clearly; it confirms $b>g$. Therefore; the color of exhaust is magenta that is complementary color of green.

9. Applied to black mist layer of Japan Alps

Many peoples believe that there is clear atmosphere on high mountains over 2700 m. It was a fact; however, after 2007, the air of high mountains is contaminated gradually.

Owner of mountain cottage, Hakuunso, at Tatamidaira (2702m) say that; There was no difference about brightness of stars at Tatamidaira, Marishiten (2872m), and Kengamine (3025m) formerly. But, we don’t feel pure star sky at Tatamidaira recently. There are cases that

Tatamidaira is cloudy but Kengamine is fine. We think *there is a dim layer between 2.7 and 2.8 km*. Former days, Tatamidaira is a famous spot to make shooting stars; the period is autumn, when moving anticyclone is growth. However, during the period, it is not clear sky recently. Sky photographers select summer days, when anticyclone is growth on Pacific Ocean.



Figure 9. Visual image of black mist layer on Hodaka and Yari at 7:25 JST in 2013.9.11. Nikon D7100, ISO=100, 1/2000s with micro Nikkor 105mmF5.6.

We found black mist layers for west direction of Norikura Marishiten peak, at Sep. in 2011. Moreover, we found the black mist layers on Hodaka and Yari mountains at Sep. in 2013. The black mist is displayed in Figure 9.

This is normal Jpeg developing image. We use the original RAW 14-bits data, and research the mist layer.

At first, we make contour mapping for whole pixels of R-elements, and get Figure 10. For G- and B-elements give almost same images.

Two dimensional FT whose size is 721×721 pixels and expansion waves are 70 per one direction. There are two layers, and the lower one is turbulence by Yari-mountain.

Color of the black mist layer is researched by same approach of section 7; and we get Figure 12.

The layer looks very weak black in $\{b/r\}$; it is tested by increasing signal-multiply until 5. It seems white band in $\{g/r\}$, and is clearly black in $\{b/g\}$. It indicates $g > r - b$; *i.e.*, the color is green. Therefore, the black mist layer has different color against volcano exhaust gas. It is not last status of the exhaust.

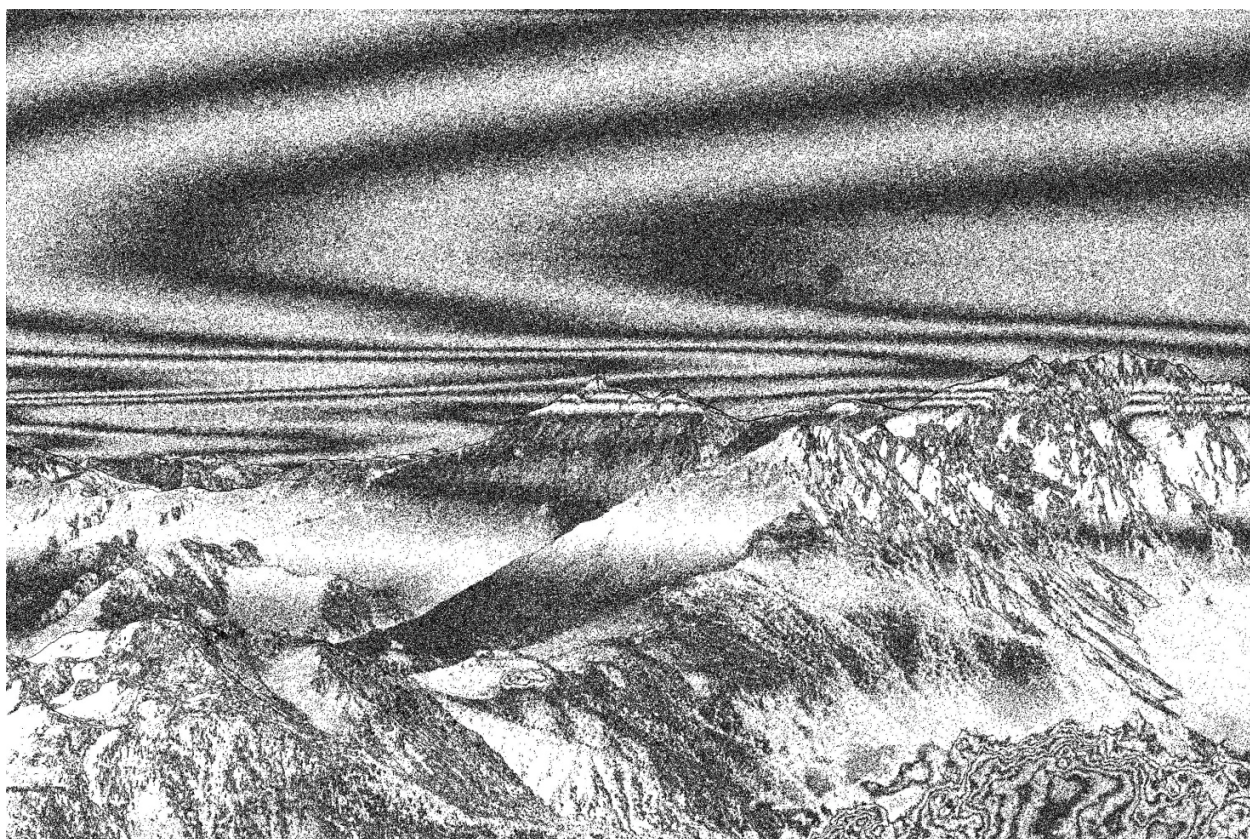


Figure 10. Black mist layers on Hodaka and Yari mountains at 7:25 JST in 2013.9.11. The contour lines ($d=0.1$) shows same brightness of R-light (600-650nm), which is photographed by prof. T. Yagi, using Nikon D7100, ISO=100, 1/2000s with micro Nikkor 105mmF5.6.

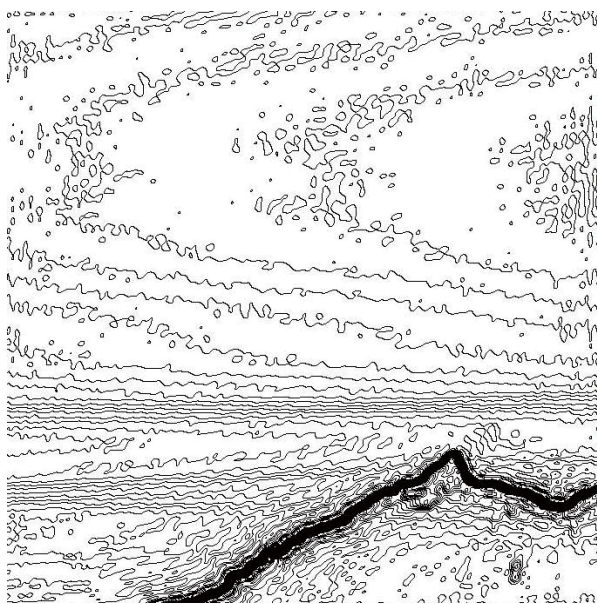


Figure 11: Contour map of black mist layer on Yari (3180 m).

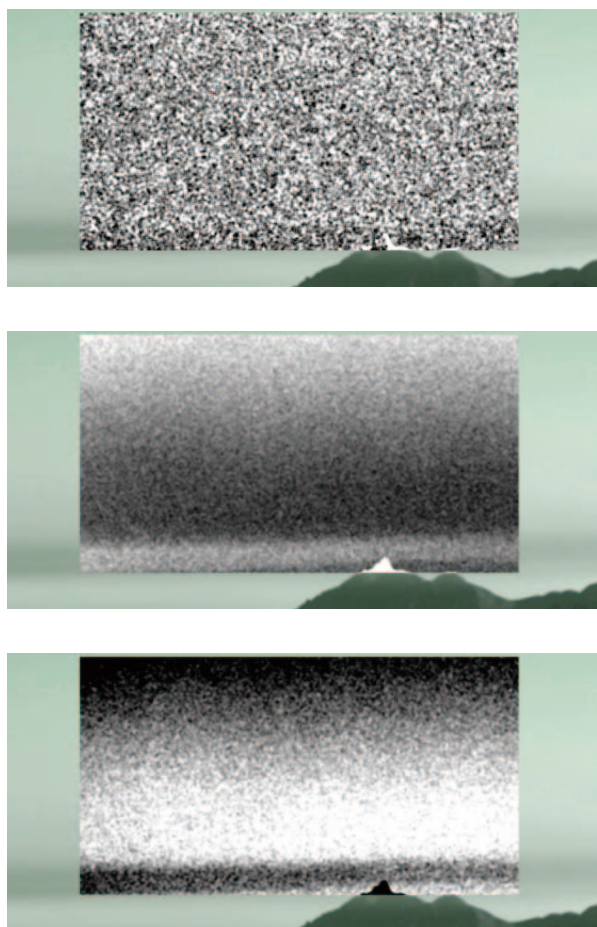


Figure 12: From top to bottom, 3 images are {b/r, g/r, b/g} of black mist layer on Mt. Yari (3180m). Intensity of images is amplified by 5, 1.7, 3 times, respectively. The color-ratio image is superimposed in a original image. The ratio part is monochrome.

10. Conclusion

Digital cameras have a potential of huge color world beyond human being. We wish to search the world and get new image of SPM in the atmosphere. We adopt color-ratios, contour map, two dimensional Fourier Transformation. Using these approaches, we research volcano exhaust and black mist layer on Yakadake and Yari mountains, and show the density distribution maps and hidden color information. Considering the color, the gas and mist are different chemical characters. The result indicates digital cameras are used as a kind of measurements for the colorimetric analysis.

Their expressions in order to process RAW data of digital cameras are published. By using the expressions, anyone try to research the RAW data. The approach is not restricted for dusts. We wish that the techniques are used for many researchers.

The contents of this report are published at 2016.9.20, the 2nd work shop for information and education in University of Edogawa.

References:

- [1] Kozo NAKAMURA, “Clouds and the Modeling (in Japanese)”, JAMSTEC Seminar #35, 2005.7.9, https://www.jamstec.go.jp/frsgc/jp/sympo/2005/seminar/35/YES_Seminar_Jul09.pdf.
- [2] T. YAGI, J. KAMBE, E. NAKAYAMA, U. NAGASHIMA, T. AOYAMA, “Air Pollution Observed at the Marishiten Peak (Elevation 2872 m) in Mt. Norikura”, Journal of Computer Chemistry, Japan, Vol. 12 (2013) No. 2.
- [3] standard RGB, “Color space” in Wikipedia, https://en.wikipedia.org/wiki/Color_space
- [4] Joint Photographic Experts Group, “Overview of JPEG”, <https://jpeg.org/jpeg/>
- [5] T. SEKIYAMA, “Observation of Aerosol from the Space (in Japanese)”, Technical report in JMA, <http://www.mri-jma.go.jp/Dep/ap/ap1lab/member/tsekiyam/files/satellite2011.pdf>
- [6] J. KAMBE, U. NAGASHIMA, T. KOZUMA, E. NAKAYAMA, T. AOYAMA, “Digital Photo Analysis of Fine Sky”, Journal of Computer Chemistry, Japan, Vol. 8 (2009) No. 4.

- [7] Shinichi OISHI, "Fourier Transformation (in Japanese)", Iwanami Co. Ltd., 1989.6.13, ISBN-13: 978-4000077767.
- [8] Yuji IZAWA, "Window Function (in Japanese)", private technical report in University of Shinsyu, <http://laputa.cs.shinshu-u.ac.jp/~yizawa/InfSys1/basic/chap9/index.htm>.